EERI Earthquake Reconnaissance Team Report:

M7.1 Puebla, Mexico Earthquake on September 19, 2017

Deborah Weiser, Jeffrey Hunt, Ezra Jampole, and Maurizio Gobbato

February 2018

A product of the EERI Learning From Earthquakes Program

1. RECONNAISSANCE TEAM OVERVIEW

On September 19, 2017, a 48-km deep, magnitude 7.1 earthquake occurred near Ayutla, Puebla, Mexico. Two weeks after the earthquake, a multidisciplinary team, representing three different companies in partnership with EERI, travelled to Mexico City to study the impacts of the earthquake. The team conducted field reconnaissance from October 3-8, 2017. This report summarizes the team's observations during their reconnaissance trip. It is part of a growing collection of information that the EERI staff, reconnaissance team, and community have stored on a detailed virtual clearinghouse website (EERI, 2017a, 2017b, and 2017c).

Building Damage Sampling Team (BDST) members included:

- Dr. Deborah Weiser, Geologist and Customer Success Engineer at One Concern; BDST co-leader
- Dr. Jeffrey Hunt, P.E., EERI Learning From Earthquakes Executive Committee Member and Managing Engineer, Buildings and Structures Practice at Exponent; BDST co-leader
- Dr. Ezra Jampole, Associate, Buildings and Structures Practice at Exponent
- Dr. Maurizio Gobbato, Principal Catastrophe Risk Modeler at Risk Management Solutions

The four core BDST members led a vigorous mapping of building performance across Mexico City, resulting in invaluable data to inform the understanding of Mexico City's vulnerabilities. The BDST was supported by academic and professional partners, many of whom were local to Mexico City.

The team's technical objectives for this reconnaissance effort included:

1. Conduct a high-level building performance review,
2. Focus data collection on buildings with close proximity to a nearby ground motion recording station, in order to more closely correlate the observed damage with earthquake shaking intensity,
3. Document building response for a diverse group of buildings,
4. Assess both damaged and undamaged structures, and
5. Collect at least 700 data points.

2. SEISMICITY

2.1. Seismicity and Geotechnical Setting

The Mw 7.1 Puebla, Mexico Earthquake of 19 September 2017 (18:14:38 UTC) was located at a depth of 48 km with epicentral coordinates 18.550°N, 98.489°W – approximately 1 km west of Ayutla in central Mexico (USGS, 2017). The epicenter was located approximately 150 km southeast of Mexico City. The earthquake occurred as a result of normal faulting near the plate boundary of the Cocos Plate and the North American Plate. The USGS indicates that the earthquake was likely an intraplate event within the Cocos plate because of the location, depth, and normal faulting mechanism (USGS, 2017). The earthquake occurred on the 28th anniversary of the 1985 M8.0 Michoacan earthquake, which occurred as a result of thrust faulting and killed between 5,000 and 10,000 people in Mexico City.

Much of Mexico City is built on a former lake that was gradually filled in by the Spanish to control flooding after their conquest of the Aztec capital of Tenochtitlan. The lakebed area is thus characterized by extremely soft soil, with the fundamental soil period at a particular site dependent on the depth of deposits. Figure 1 shows soil period contours (Gomez and Garcia-Ruiz, 1988) and shading (from Colegio De Ingenieros Civiles De Mexico, or CICM) for the Mexico City Area. The shaded regions correspond to the areas of the former lakebed. Recording stations visited by the BDST are also shown on the map as black dots.

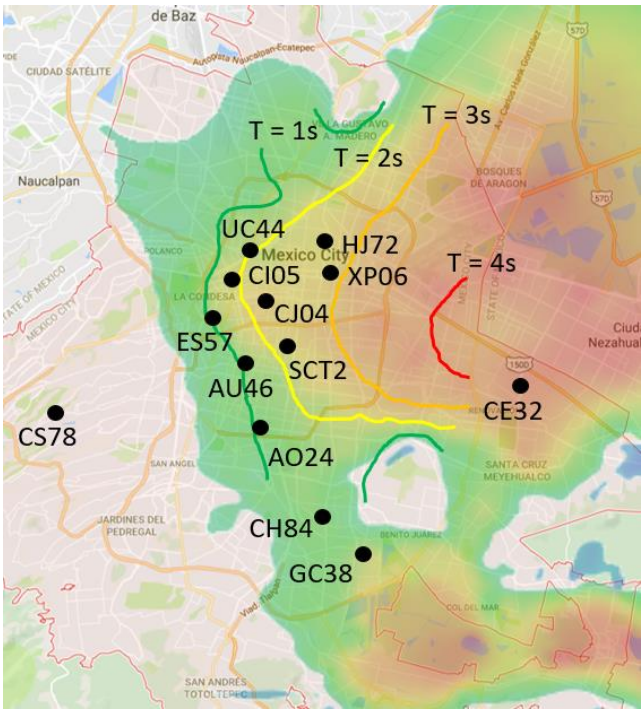

Figure 1. Soil period contours (from Gomez and Garcia-Ranz, 1988) and shading (from CICM) with recording stations visited by the Building Damage Sampling Team over a map of Mexico City (Google).

The soil conditions in Mexico City are historically divided into three main zones: Firm Zone (Zone I), Transition Zone (Zone II), and Lakebed Zone (III) (Rosenblueth, 1979). The 2004 Mexico City building code has further divided the Lakebed and Transition Zone into subsections (Gobierno del Distrito Federal Mexico, 2004). Figure 2 shows the soil zones from the 2004 code. Figure 3 shows the evolution of the design response spectra for Mexico City in the three main zones from the 1976 code, the 1987 code (enacted after the 1985 earthquake), and the 2004 code.

The shape and amplitudes of the design response spectra have remained similar for the firm zone from 1976 to 2004. The constant acceleration/peak portion of the 2004 design response for the firm zone spectrum at 0.17g extends to slightly longer periods compared to the 1976 and 1987 codes. The peak spectral accelerations in the 1987 and 2004 design response spectra for the Transition Zone and the Lakebed Zone increased significantly (50-80%) from the 1976 code. These revisions were made as a result of observations of performance during the 1985 earthquake. The peak design spectral acceleration is significantly higher in the Lakebed Zone than the Transition Zone and Firm Zone.

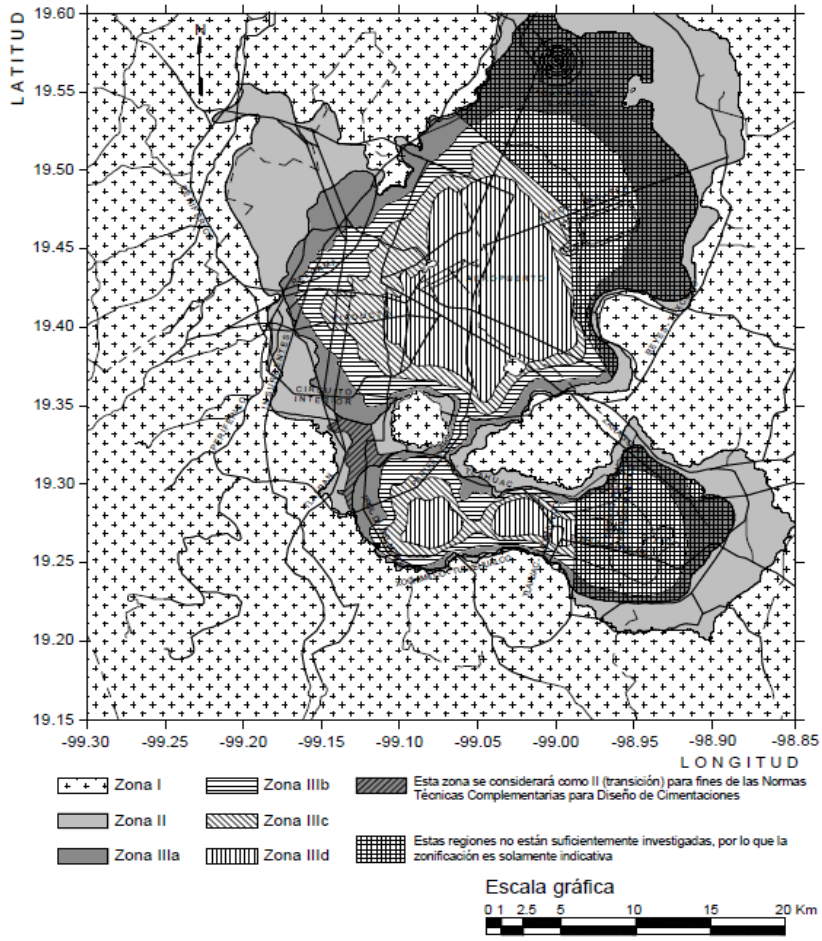

Figure 2. Soil zones from the 2004 Mexico City building code.

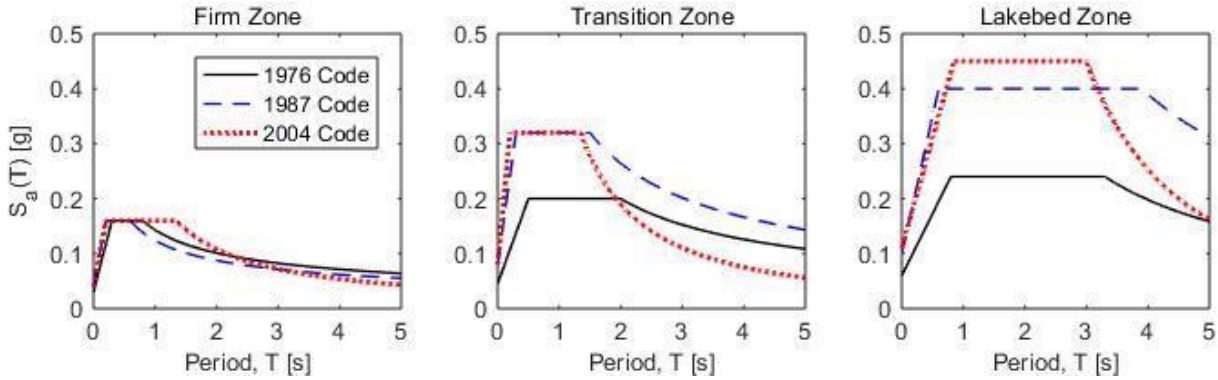

(a) *(b)* *(c)*

Figure 3. Building code design response spectra in Mexico City for 1976, 1987, and 2004 in the: (a) Firm Zone; (b) Transition Zone; and (c) Lakebed Zone. The Lakebed Zone for the 2004 code is zone IIIb.

2.2. Response Spectra of Recorded Ground Motions and Comparisons

Figure 4 shows a map of estimated peak ground acceleration (PGA) in Central Mexico from the September 19, 2017 earthquake. PGA intensity was the greatest near the earthquake's epicenter, which is indicated by the star in the center of the map, with a peak PGA of approximately 150 cm/s^2. As the seismic waves travel out farther from the epicenter, the amplitude of shaking attenuates and the PGA decreases. However, as the waves encounter the Lakebed and Transition Zone soils in Mexico City, the PGA increases to greater than 100 cm/s^2 as a result of site soil amplification effects.

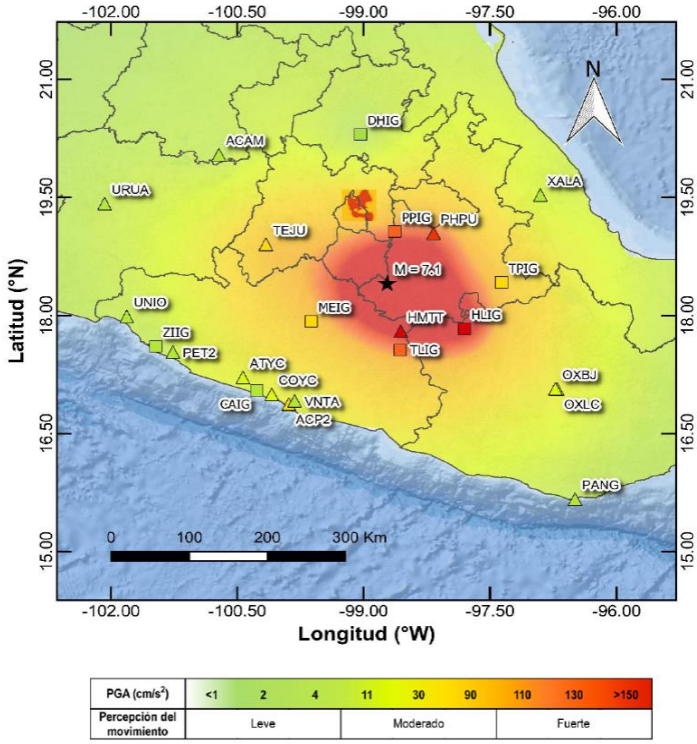

Figure 4. Peak ground acceleration map of Mexico during the 19 September 2017 earthquake (Source: Instituto de Ingenieria UNAM, 2017*).*

Figure 5a shows the geometric mean 5% damped response spectra of as-recorded orthogonal horizontal components of the ground motion at the stations visited by the EERI team, and Figure 5b shows the 5% damped vertical response spectra for the sites. The horizontal spectra are characterized by peaks over a narrow band of periods, indicative of the approximate soil period at the site. Peaks of the response spectra in the Transition Zone typically occur at a period between 1 and 2 seconds, with amplitudes of approximately 0.5g. Table 1 summarizes numerous ground motion intensity measures such as PGA, peak ground velocity (PGV), incremental ground velocity (Vgi), cumulative absolute velocity (CAV), Sa_average between 1 and 3 seconds, the peak period at the peak spectral acceleration, the peak spectral acceleration, and the significant duration (D5-75 and D5-95). The PGA in the Lakebed and Transition Zones is typically between 0.1 and 0.15g, with one recording station measuring PGA = 0.19g.

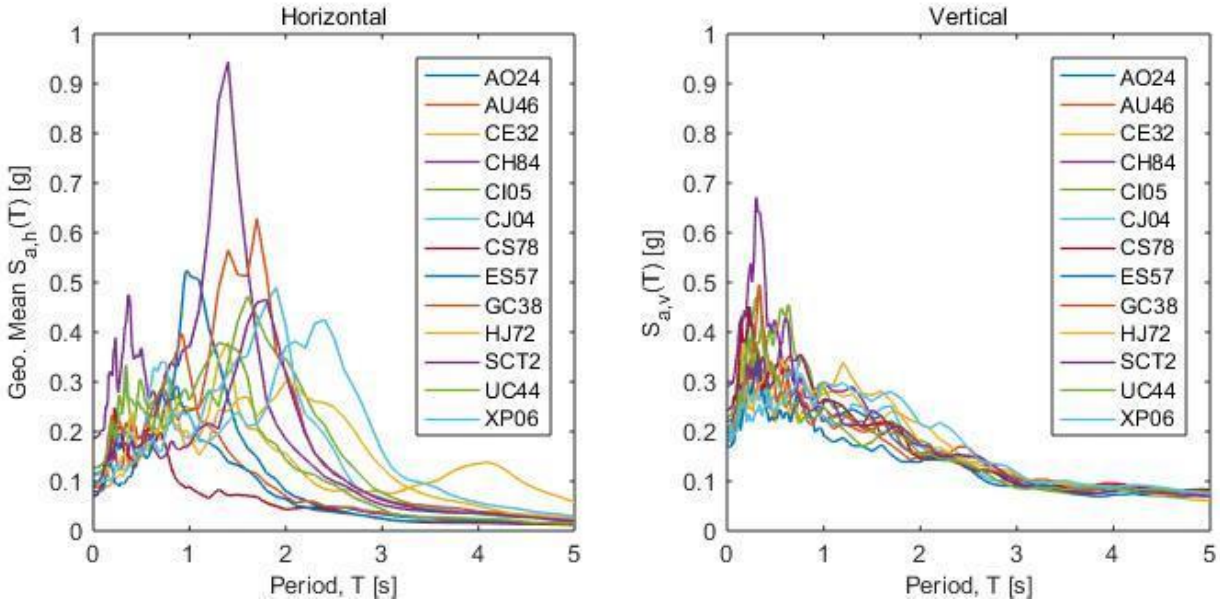

(a) *(b)*

Figure 5. Response spectra at visited recording stations: (a) Geometric mean of orthogonal horizontal components; and (b) vertical component.

Table 1. Ground motion intensity measures for recording stations near structures visited by the Building Damage Sampling Team.

Recording Station	CIRES Classification	N. Latitude	W. Longitude	GeoMean Horizontal PGA [g]	Vertical PGA [g]	GeoMean PGV [cm/s]	GeoMean Vgi [cm/s]	GeoMean CAV [cm/s]	GeoMean Sa_average (1-3s) [g]	Period at Peak Sa [s]	Peak Sa [g]	D5-75 [s]	D5-90 [s]
AO24	Transition	19.358	99.1539	0.12	0.05	17	33	1185	0.16	0.97	0.52	14	32
AU46	Transition	19.3832	99.1681	0.09	0.03	14	26	993	0.11	0.92	0.40	22	38
CE32	Lakebed	19.3858	99.0537	0.08	0.04	22	37	1254	0.16	1.40	0.38	20	48
CH84	Lakebed	19.33	99.1254	0.19	0.09	34	64	2146	0.31	1.40	0.94	12	30
CI05	Lakebed	19.4186	99.1653	0.12	0.05	25	46	2021	0.26	1.60	0.47	30	50
CJ04	Lakebed	19.4098	99.1566	0.11	0.04	28	52	1855	0.25	1.90	0.49	30	51
CS78	Firm	19.3656	99.2262	0.07	0.06	8	13	544	0.05	0.22	0.25	12	28
ES57	Transition	19.4017	99.1775	0.08	0.03	12	21	895	0.09	0.86	0.29	22	40
GC38	Lakebed	19.316	99.1059	0.13	0.04	31	58	2098	0.29	1.70	0.63	22	51
HJ72	Lakebed	19.4251	99.1301	0.10	0.04	24	41	1608	0.23	2.00	0.30	27	69
SCT2	Lakebed	19.3928	99.1474	0.09	0.04	25	44	1744	0.23	1.80	0.47	37	49
UC44	Lakebed	19.4337	99.1654	0.13	0.04	19	37	1324	0.19	1.30	0.38	20	40
XP06	Lakebed	19.4198	99.1353	0.10	0.03	31	57	2252	0.28	2.40	0.43	40	91

Figure 6 compares the intensity measures for the recording stations visited by the BDST (in red) and the remaining 49 recording stations in the CIRES network (black). There is strong correlation between the PGA and energy in individual pulses (PGV or Vgi), between the peak ground acceleration and the average spectral acceleration between 1 and 3 second periods, and between the PGA and the CAV. It is noted that the team visited stations that are representative of the full range of intensity measure values.

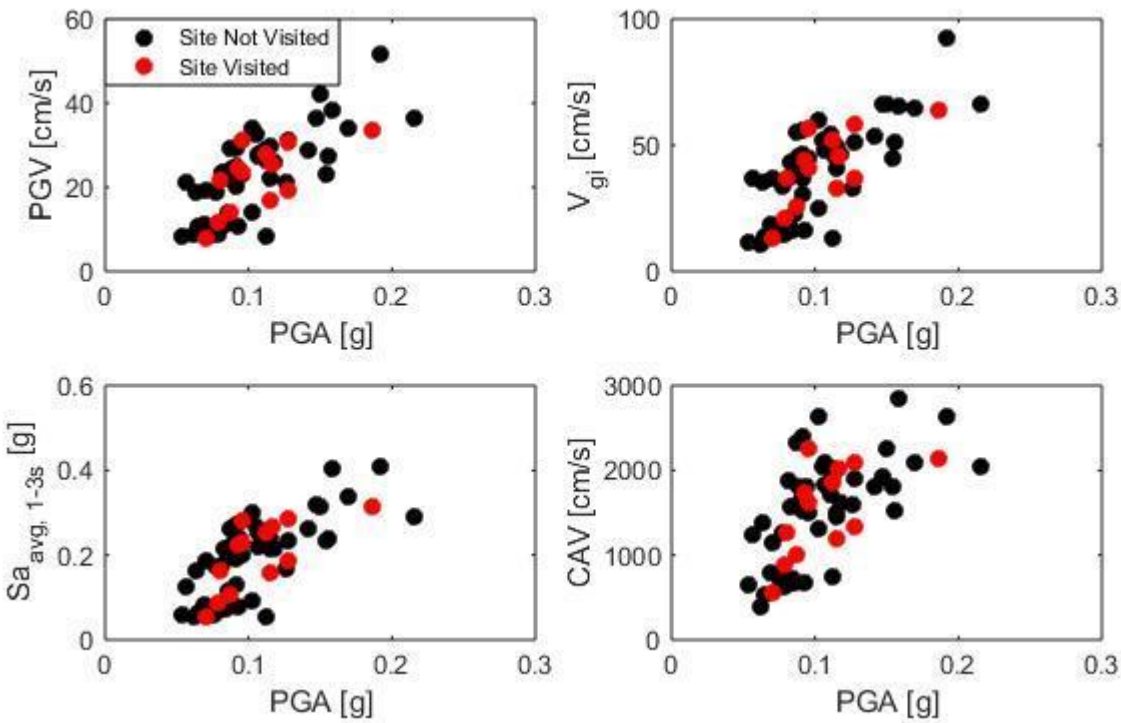

Figure 6. Geometric mean Intensity measures at recording stations in Mexico City (CIRES network).

3. DATA COLLECTION

Before setting out for fieldwork, the BDST began discussions with US-based professional earthquake engineering associations. There was a great deal of interest in reconnaissance work, from many scientists, engineers, and private companies. EERI coordinated many conversations and conference calls, which illuminated the scope of the US-based groups' site response. EERI also helped coordinate communication with Mexican colleagues, as not to overwhelm them with requests from international teams. These pre-field work discussions provided valuable situational awareness, tips for travel within Mexico, and opportunities for collaboration and shared knowledge.

The team conducted damage surveys for all buildings, both damaged and undamaged, located within a specific radius around a selected strong motion recording station. As shown in Figure 1, observed buildings were grouped around 13 different recording stations, which were selected to capture different ground motion intensity levels, shaking durations, building details (primary use, footprint, number of stories, and construction type), and soil characteristics (on lakebed, off lakebed, and on transition soils). When choosing stations, sites with similar ground motion and duration characteristics, which were located in different locations relative to the lakebed/transition soils, were considered. Most buildings within approximately 1,000 feet of the selected stations were surveyed; data were also collected for structures not within this boundary. The team assumed that the shaking recorded at a station was an appropriate proxy for most structures within a 1,000 foot radius from the station. Farther from recording stations, correlations of shaking intensity between the recorded motion and the building site are decreased, and this decrease has been shown to vary with natural vibration periods (Goda and Hong, 2008).

A mobile phone application, customized by the BDST, was used to collect field data for each building, including photographs, GPS coordinates, structural system, primary building use, number of stories, damage severity, age of construction, and other performance impactors. Damage severity was classified into five damage states, DS 0-4. The damage states are as follows:

- DS 0 – no observed earthquake-related damage. No repairs would be required.

- DS 1 – minor (mostly cosmetic) damage. See example in Figure 7. This damage typically involves minor cracks in masonry or concrete elements and/or minor damage to exterior non-structural components (ornamentation, facades, windows, etc.). Repairs would be localized and consist of patching/painting cracks and repairs to non-structural components.

- DS 2 – moderate structural damage. See example in Figure 8. This damage typically involves wider cracks and spalling in masonry or concrete elements. Cracks can be repaired in place by routing and repointing grout masonry walls, and patching/epoxy injecting cracks in concrete walls.

- DS 3 – severe damage. See example in Figure 9. This damage involves severe shear cracks in masonry and concrete elements. Residual drift of a story may be present. Repair of damaged elements in place may not be economical.

- DS 4 – partial or complete collapse. See example in Figure 10.

Figure 7. Example of damage state 1: minor (mostly cosmetic) damage.

Figure 8. Example of damage state 2: moderate structural damage.

Figure 9. Example of damage state 3: severe damage.

Figure 10. Example of damage state 4: partial or complete collapse of structure.

The BDST observed 713 buildings. A map of these buildings is provided in Figure 11, along with a close-up of a typical group of observations around a strong motion recording station.

At two stations, observed structures were clustered nearby, but at some distance from the station. Near many stations, additional buildings were observed that were not clustered around the station or other observed/tagged buildings. These additional buildings were tagged and are part of the dataset because they are generally more heavily damaged, but should not necessarily be included in statistics of buildings around recording stations because the full population of buildings was not sampled around these additional buildings.

Figure 12 shows the distance of each building observed to the nearest recording station, and approximate probability density functions to illustrate the distance of most of the buildings observed around a recording station to that recording station. Black horizontal lines indicate the cutoff distance for buildings that are part of the full population sample cluster of buildings. Dots below the black horizontal line indicate buildings that were observed as part of the full population cluster of buildings near the recording station. Dots above the black horizontal line indicate buildings that were observed near the recording station but were not part of the full population sample. The total number of buildings that are part of the full-population cluster is given next to the recording station name on the horizontal axis.

Table 2 summarizes the type of buildings typically in the population around each recording station, the radius for the full population sample, the number of observed buildings in that radius, and the number of buildings within the radius that were observed to have each damage state (DS).

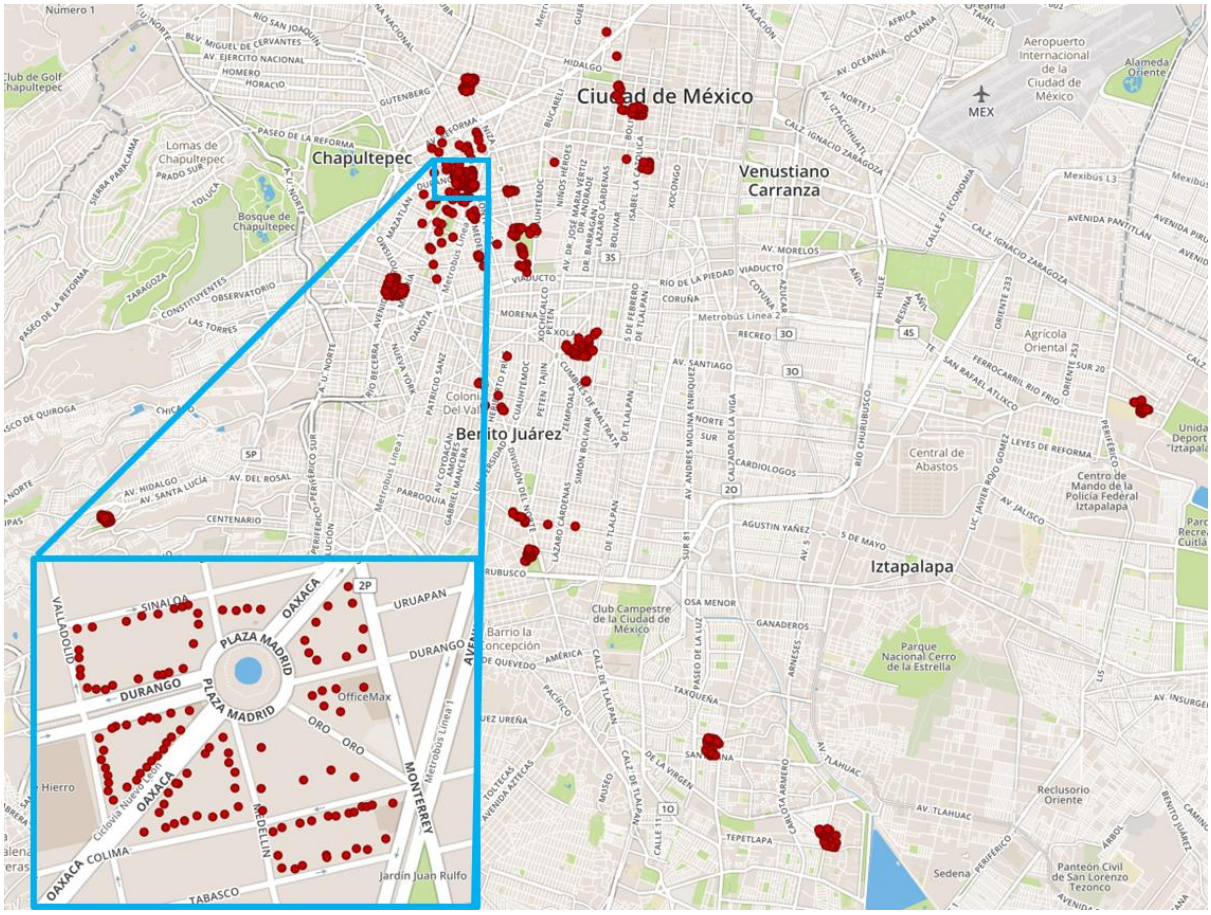

Figure 11. Map of the 713 observed buildings in Mexico City. Inset at lower left shows one of the clusters of buildings around a strong motion recording station.

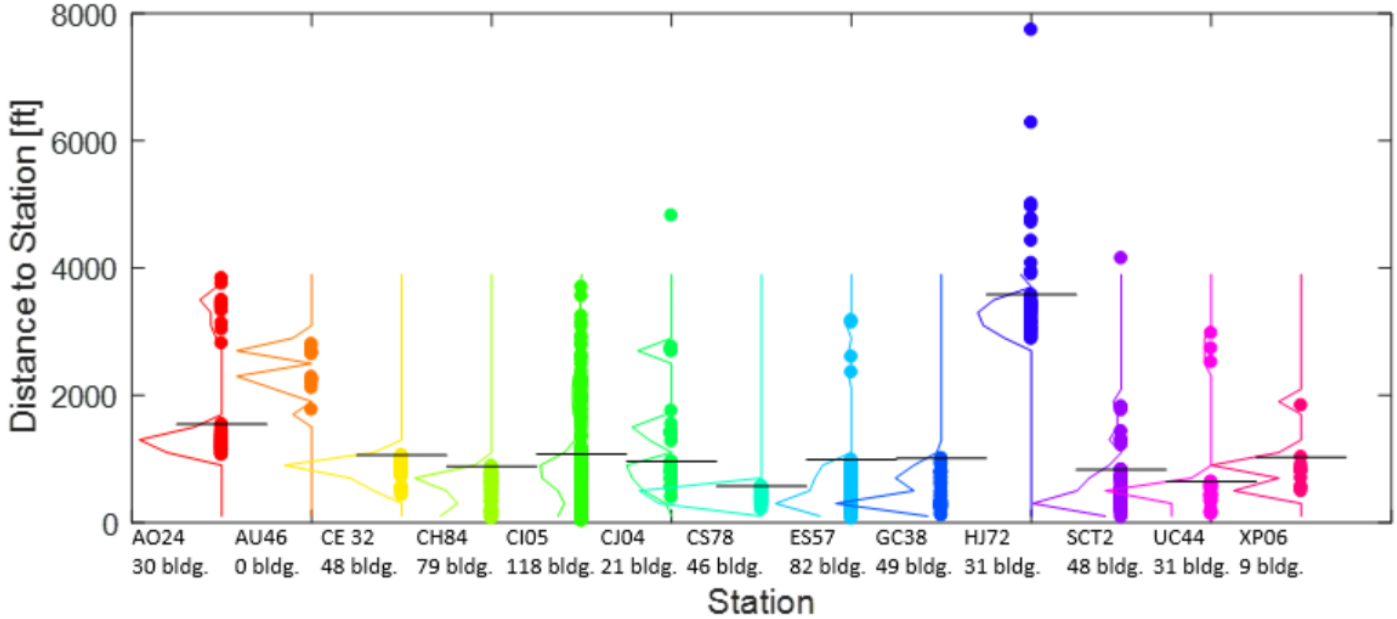

Figure 12. Distance of buildings to recording stations. Clusters are indicated as below the horizontal black line for the recording station.

Table 2. Summary of buildings observed at each recording station visited that are part of the full-population clustered sample.

Recording Station	Description of buildings around station	sample w/in radius [ft]	# of structures w/in radius	DS 0	DS 1	DS 2	DS 3	DS 4
AO24	2-5 story row apartments/houses	1546	30	28	2	0	0	0
AU46	5-10 story apartment buildings	0	0	0	0	0	0	0
CE32	2-3 story apartments and condos	1057	48	48	0	0	0	0
CH84	2-4 story row houses, some shops, school, many houses built in the 90s	883	79	68	8	2	0	1
CI05	5-10 story businesses, school	1076	118	79	35	4	0	0
CJ04	4-6 story apartment buildings, govt building	961	21	19	2	0	0	0
CS78	2-3 story row houses, 5 story apartment complexes	571	46	46	0	0	0	0
ES57	3-5 story business and apartment buildings, school	987	82	69	11	2	0	0
GC38	4 story apartment buildings, 2-4 story row houses	1008	49	47	2	0	0	0
HJ72	commercial buildings 5-10 stories	3581	31	22	8	0	1	0
SCT2	commercial/government/large apartment buildings, so 5-6 story row apartments/businesses	830	48	43	3	1	1	0
UC44	government, commercial, school, 2-10 stories	642	31	23	8	0	0	0
XP06	government buildings, commercial	1027	9	8	1	0	0	0

An obvious application of the dataset is to create fragility curves for damage states, which could depend on intensity, building type, building height, and the numerous performance impactors previously highlighted. A simple case is shown in Figure 13, in which PGA is used as the intensity measure and buildings are not parsed by construction type, age, etc. Each point represents the probability of exceeding a damage state at each recording station, for the PGA at the recording station. There is no obvious trend in the plotted data because there is not enough information contained within PGA to assess the probability of damage (i.e. PGA alone is a poor predictor of damage state at a particular site in Mexico City).

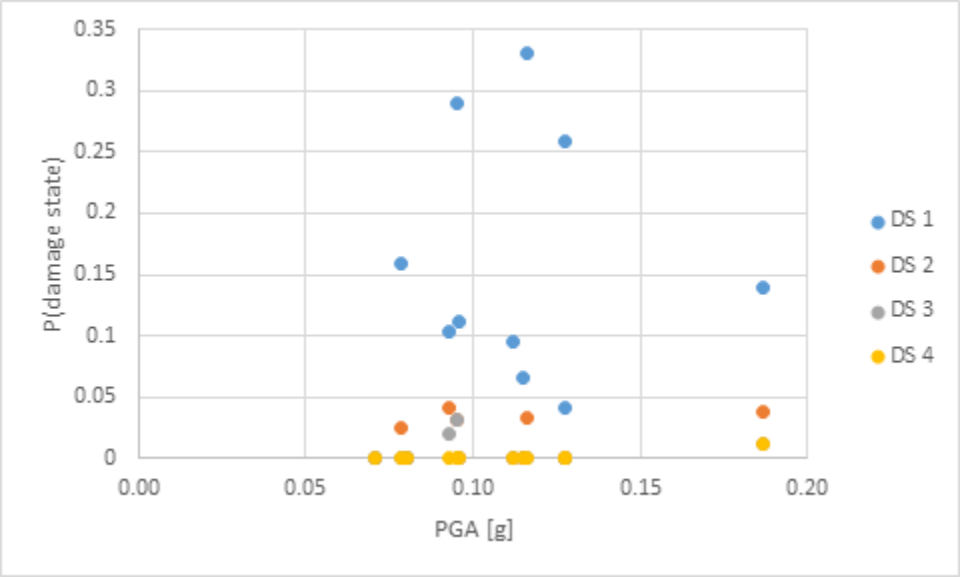

Figure 13. Probability of exceeding a damage state at each recording station vs. PGA.

4. DAMAGE TO STRUCTURAL COMPONENTS

During the 6-day reconnaissance period, the team surveyed 713 buildings clustered around key recording stations as discussed earlier. A total of 148 buildings were classified by the team as either DS1 or DS 2, and a total of 38 buildings were classified as either DS3 or DS4. The majority (about 75%) of the severely damaged buildings (DS3 and DS4) were between 4- and 9-stories tall, as illustrated in Figure 14(a). A different trend is observed for the two lower damage states (DS1 and DS2). Approximately half (about 45%) of buildings classified as either DS1 or DS2 were between 1 and 3 stories, 20% were in the 4-to-6 stories height band and another 20% were between 7 to 9-stories tall.

Most of the surveyed buildings (about 80%) were categorized as reinforced concrete (RC) with unreinforced masonry (URM) infills. This category can either refer to RC frames with URM infills or RC columns with waffle or flat slabs and URM infills. Additionally, 10% of the surveyed buildings were identified as RC moment resisting frames (RC-MRF), 5% as URM (typically built using either concrete blocks or clay-fired bricks), 4% as RC shear wall systems and the remainder (3%) as either Steel frames, light metal frames or precast concrete. The predominant structural system mentioned above (RC with URM infills) is still widely used in new constructions in Mexico City, especially for mid-rise buildings. URM is used for new construction in rural parts of Mexico. As illustrated in Figure 14(b), the distribution of the damaged buildings (blue and red bars) by construction type closely follows the distribution of construction type of the entire surveyed stock (green bars). Over 90% of the buildings classified as either DS3 or DS4 were identified as RC with URM infills. Severe damage in URMs and RC-MRFs was very limited due to either the predominately low height in the case of URMs or the more recent year of construction for the RC-MRFs encountered in our survey.

60% of the surveyed buildings in either DS3 or DS4 were multi-story multi-family residential buildings, 30% were multi-story office or commercial buildings, and the remaining 10% served either governmental or lodging functions.

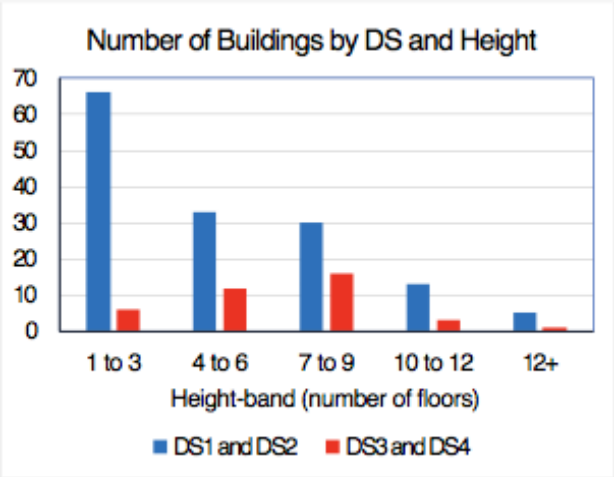

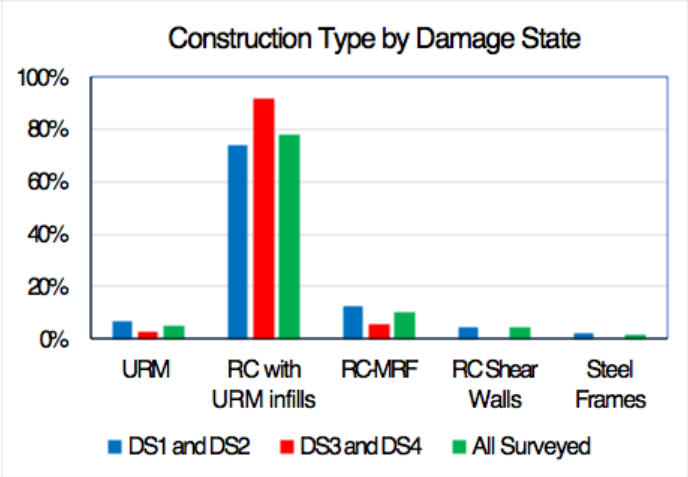

(a) (b)

Figure 14. (a) Number of buildings by damage state and height-band; (b) Percentage of buildings by construction type and damage state.

Building structural and geometric characteristics ("performance factors") had an important influence on severity of damage observed. Due to the density of buildings in Mexico City, the potential for pounding was the performance factor observed the most frequently, as highlighted in Figure 15(a). About 60% of the undamaged buildings, 80% of those in damage states DS1 and DS2, and 90% of those in either DS3 or DS4 were susceptible to or impacted by potential pounding effects. It is also important to emphasize how the percentage of buildings impacted by pounding increases with the observed damage severity: from about 60% for undamaged buildings to 90% for buildings in either DS3 or DS4. Even more pronounced is the increase of the percentage of buildings impacted by a soft story: from 15% for undamaged buildings to 50% for buildings in either DS3 or DS4.

Additionally, as shown in Figure 15(b), the number of performance factors impacting a given building has a clear influence on the overall seismic performance. About 70% of the undamaged buildings were impacted by at least one performance factor and about 30% by at least two factors. All buildings with observed DS3 or DS4 were impacted by at least one performance factor and about 55% of them were impacted by at least two. In other words, buildings in either DS3 or DS4 were approximately twice as likely to have at least two performance factors than buildings in DS0.

Figures 16(a) through 16(c) provide a split by height-band view of the data shown on Figure 15(b). Similar trends are observed across the three different height-bands with the percentage of buildings (in each height-band and for a given minimum number of impacting performance factors) increasing as the severity of the observed damage state increases.

A comprehensive update to the Mexico City Building Code (NTCS-87, 1987) was introduced in 1987, in response to the widespread damage and the lessons learned following the 1985 M_w8.0 Michoacan Earthquake. The 1987 code contained important improvements, including the requirement to design buildings located in certain zones to withstand higher shaking intensities. The team found that about 60% of the surveyed buildings appeared to have been constructed prior to 1987. Additionally, with focus on the surveyed building within either DS1 or DS2 damage state, about 50% were estimated to be built prior to 1987. Similarly, with focus on the surveyed buildings within either DS3 or DS4 damage state, about 70% were estimated to be built prior to the introduction of the 1987 building code.

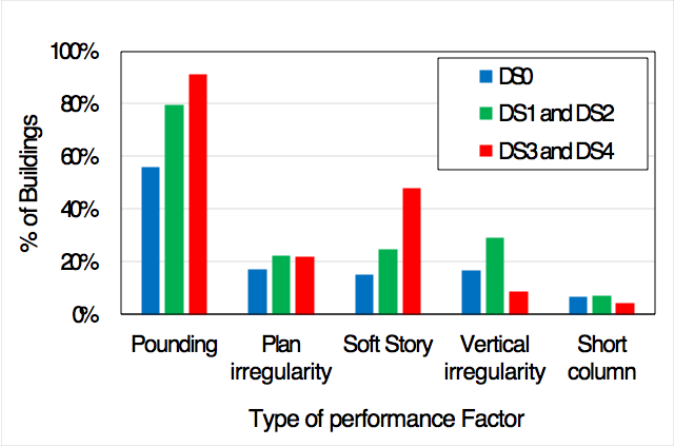

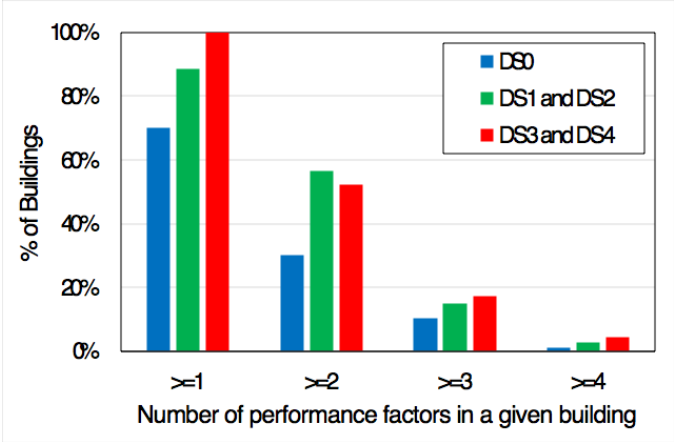

(a) (b)

Figure 15. (a) Percentage of buildings, by damage state (or damage state group), impacted by the most frequent performance factors observed during the survey; (b) Percentage of buildings, by damage state (or damage state group), as a function of the number of performance factors observed.

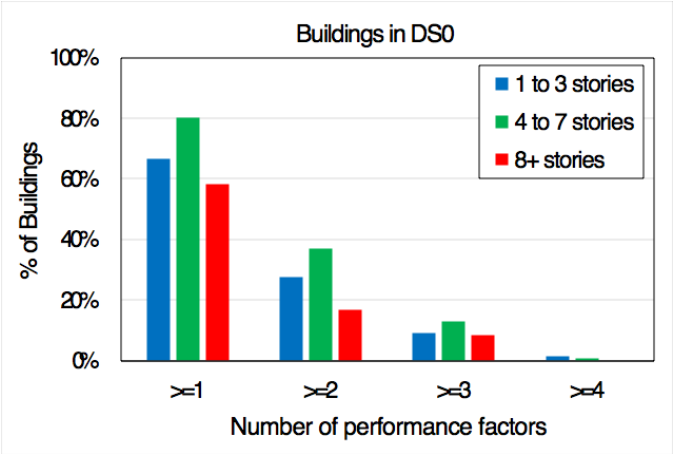

(a)

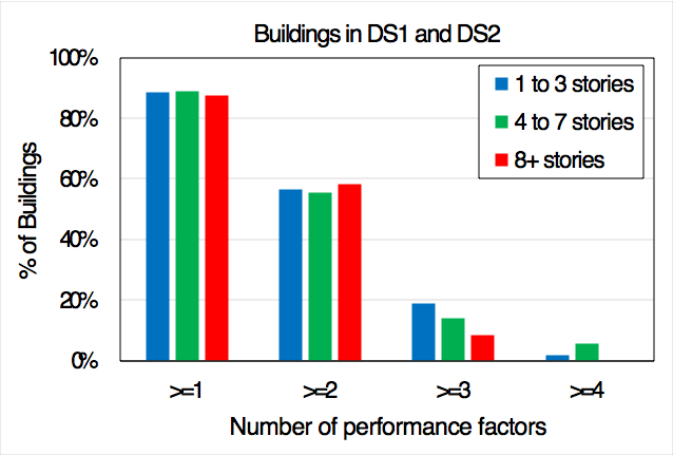

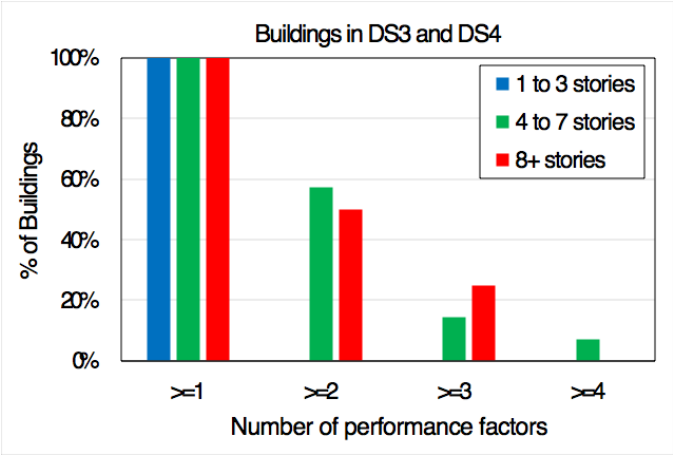

(c) (d)

Figure 16. (a) Percentage of buildings impacted by at least one performance factor as a function of damage state (or damage state group) and height-band; (b)-(d) Percentage of buildings, by damage state (or damage state group) and height-band, as a function of the number of performance factors observed.

The team observed that about 60% of the building categorized as either DS3 or DS4 were end-buildings[1] and this percentage increases to 65% focusing solely on DS4. Considering that only 33% of all the buildings surveyed were categorized as an end-building, it can be inferred that an-end building was between three to four times more likely to sustain damage during the 2017 M7.1 Puebla earthquake. The primary reason end buildings are more susceptible to higher damage is that they are not laterally restrained or confined by adjacent buildings on both sides during an earthquake, i.e. end buildings serve as a fuse in a row of buildings because they are only restrained on one side in a particular direction, while buildings in the middle of a row are restrained on both sides. Another reason corner buildings can be especially vulnerable is that they often have more and/or larger openings than other buildings; for example, corner buildings typically have commercial shops on their ground floors with windows or doors for easier street access, on both of their street-facing sides.

Lastly, the team found that about 70% of all the surveyed buildings were prone to suffer from pounding during an earthquake event. The ratio increases to 80% among the buildings categorized as either DS1 or DS2, and to 90% for those categorized as either DS3 or DS4. The most severely damaged buildings often had buildings of different heights on either side and/or floor levels that did not align between adjacent buildings, indicating that pounding significantly impacted performance.

4.1 Unreinforced Masonry Buildings

The team surveyed 35 URM buildings (out of a total of 713); among them, 23 were undamaged, 11 were classified as either DS1 or DS2 and only one as DS4. This last URM building is shown in Figure 17 and it suffered a partial collapse during the earthquake. The second-story structural and partition walls as well the roof partially collapsed. On the other hand, the first-story structural elements were still standing. This URM construction was a pre-1987 residential corner-building with plan irregularity and potential pounding from the adjacent buildings.

(a)

(b)

[1] In this study, an “end building” refers to a building that is not laterally restrained/confined on one side in a row of buildings. An end building can be a corner building at the end of a row of buildings, or a building with an empty lot on one side.

(c) (d)

Figure 17. Structural damage on a partially collapsed 2-story URM residential building located at (lat., lon.) = (19.4425, -99.1430). (a) and (b): Photos prior to the earthquake from Google®; (c) and (d) Photos after the earthquake.

4.2 Reinforced Concrete Moment Resisting Frames

The team surveyed 73 RC-MRF constructions (out of a total of 713); among them, 50 were undamaged, 21 were classified as either DS1 or DS2 and only two as DS3. One of the severely damaged buildings was a 4-story post-1987 construction which experienced pounding effects from the adjacent building and, after the earthquake, had clearly observable residual drift and severe cracks on the columns. The pre- and post-earthquake photos of this structure are shown in Figure 18, and it can easily be noticed the vertical splitting failure on central column of the front façade probably caused by the insufficient amount of confinement. This was a common issue observed on many of the RC-MRF damaged during the earthquake. To further validate this point, Figure 19 shows the severe structural damage on the first-floor columns of an 8-story residential RC-MRF corner-lot building. It can be noticed how lateral confinement was clearly lacking and led to longitudinal rebar buckling, and the consequent massive spalling of the concrete.

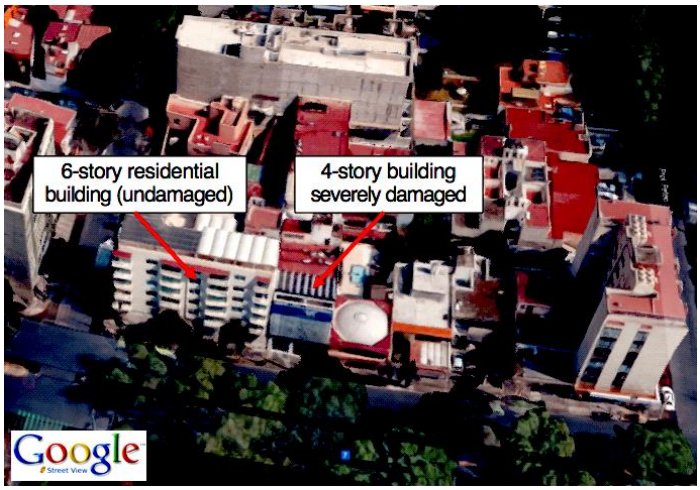

(a) (b)

(c) (d)

Figure 18. Structural damage on a severely damaged 3-story RC-MRF commercial building located at (lat., lon.) = (19.368, -99.155). (a) and (b): Photos prior to the earthquake from Google®; (c) and (d) Photos after the earthquake.

(a) (b)

(c) (d)

Figure 19. Structural damage on the first floor of an 8-story corner-lot RC residential building located at (lat., lon.) = (19.3987, -99.1589). (a): Photos prior to the earthquake from Google®; (b), (c) and (d) Photos of first-floor columns after the earthquake.

4.3 Reinforced Concrete Buildings with Masonry Infills

The team surveyed 553 RC buildings with URM infill constructions (out of a total of 713); These were either RC frames with URM infills or RC columns with waffle or flat slabs and URM infills. Among them, 409 were undamaged, 110 were classified as either DS1 or DS2 and 19 as DS3 and 15 as DS4. Additionally, among the 19 buildings categorized as DS3, 13 were built prior to 1987 (~70%); similarly, among the 15 buildings partially or completely collapsed, 13 were built prior to 1987 (~85%). The overall construction quality and level of detailing in the RC beam-to-column connections and/or in the RC bracing systems were generally poor and constitute one of the main drivers for the observed structural damage. Figure 20 gathers some examples of the observed types of damage on the RC with URM infills constructions surveyed: severe cracking and/or out-of-plane failure of the masonry infills, shear failure of the RC beams, spalling and/or buckling

of the diagonal RC braces embedded in the URM infills upon construction or retrofitting of some of the buildings. In all instances, and similarly to what was reported in the previous section for the RC-MRF buildings, the lack of proper confinement in the damaged RC members was a clear common factor among all buildings surveyed. Additionally, the poor quality of post-1987 retrofits demonstrated to be ineffective in preventing high levels of damage.

(a)

(b)

(c)

(d)

(e)

Figure 20. (a) Damage to RC beams, infill concrete blocks and exterior cladding of a 10-story RC-frame with URM infills; (b): Damage to RC beams, infill clay bricks and exterior cladding of a 11-story RC-frame with URM infills and diagonal RC bracing system; (c): Damage to the Short RC beam connections, URM infills an exterior cladding of a 8-story RC frame with URM infills; (d) and (e): Damage to the RC bracing system in a poorly retrofitted residential 9-story RC frame with URM infills.

5. DAMAGE TO NONSTRUCTURAL COMPONENTS

Damage to nonstructural components such as partition walls and facades (e.g., windows, cladding, etc.) can represent a significant portion of losses. These components are generally very sensitive to inter-story drift ratios and can control the overall building vulnerability at low seismic intensities for ductile RC-MRF or mid- to high-rise RC with URM infills structures. On the other hand, the behavior of low-rise non-ductile constructions would be affected by both structural and non-structural elements as they would both start failing at very low inter-story drift ratios; this is typically the case of low-rise URM constructions. The team observed several buildings with exterior non-structural damage to the concrete cladding on the facades, window, parapets on balconies and ornamental molding along the roof line of older buildings. In some cases, these types of non-structural damage could constitute a life hazard for the people who find themselves in the vicinity of the building during or immediately after an earthquake. Examples of observed nonstructural damage are provided in Figure 21.

Figure 21. *(a) Damage to the interior cladding, partition wall, and stairs of a x-story RC-frame with URM infills; (b): Damage to the exterior cladding of a x-story RC frame with URM infills; (c): Damage to the interior cladding of a x-story RC frame with URM infills retrofitted with RC braces; (d) Damage to windows and parapets of a x-story RC.*

6. CONCLUSIONS AND RECOMMENDATIONS

Based on their reconnaissance investigation in Mexico City approximately two weeks following the M7.1 Puebla earthquake, the EERI reconnaissance team notes the following conclusions.

Many of the observed damage states and failure modes are well known in the field earthquake engineering for vulnerable building construction such as URM infill buildings and non-ductile concrete. However, the extent of damage caused by the Puebla earthquake surprised many officials in Mexico considering that they had been planning for an event similar to the 1985 earthquake, which was higher magnitude and father away.

The rigorous data collection method of the reconnaissance team of observing all buildings within a cluster around a recording station was developed to capture the performance of both damaged and undamaged structures of all heights and construction types. The observations can then be tied to reliable seismic intensity measures from the ground motion recordings. This method provides insight into why some areas, construction types, and building heights were more heavily damaged than others.

A preliminary summary of observations from our reconnaissance is provided below:

- Damage was concentrated in buildings constructed prior to 1985.
- Damage was concentrated in buildings from 4 to 8 stories in height
- Damage was concentrated in concrete frame buildings with masonry infill, which is the predominant building system in Mexico City.
- End buildings were significantly more susceptible to damage than were buildings in the middle of a row because they are constrained on only one side in at least one direction.
- The severity of damage was binary: the damage state of similar buildings on the same block varied significantly, indicating the importance of documenting structural performance factors for buildings around the same recording station, and thus subjected to nominally similar earthquake intensity.
- The building survey described in this report provides a rich and publicly available dataset for researchers and engineers wishing to study the types of buildings that were damaged during the 19 September 2017 earthquake, and design strategies that may mitigate damage from future earthquakes.

7. ACKNOWLEDGEMENTS

Arely Acevedo at CICM set up the BDST with a briefing from CICM students and staff, equipped them with CICM structural evaluation badges, and communicated with the team while they were in the field. Special thanks to additional members who contributed to the building damage data collection process: Ricardo Ramirez and Abraham Tacho from WSP, Ted Allen from One Concern, and Daniel Fuentes from Cesar Mendez Franco S.C. (CMF).

The BDST would like to thank the residents of Mexico City (Ciudad Mexico, or CDMX) that showed compassion, curiosity, hospitality, and kindness towards our team. Their insights and experiences were very helpful, and provided a great deal of context and knowledge that we would not have otherwise learned. We greatly appreciate all who helped our team's visit to Mexico City be so successful and meaningful, a selection of whom can be seen in Figure 22. We wish CDMX residents great success in their personal and collective recovery, with a stronger, safer city emerging from their hard work.

(a)

(b)

Figure 22. (a) From left to right: Deborah Weiser, Jeffrey Hunt, Ricardo Ramirez (WSP), Ezra Jampole, and Maurizio Gobbato; (b): Deborah Weiser (left) and Daniel Fuentes (CMF, second from right) learning about local damage from two Mexico City residents.

8. REFERENCES

ASCE 7-10, 2011. Minimum design loads for buildings and other structures, American Society of Civil Engineers, Reston, VA. Copyright

Gobierno del Distrito Federal Mexico. (1987). “Normas técnicas complementarias sobre criterios y acciones para el diseño estructural de las edificaciones.”

Gobierno del Distrito Federal Mexico. (2004). “Normas técnicas complementarias sobre criterios y acciones para el diseño estructural de las edificaciones.”

Goda, K. and Hong, H.P. (2008). “Spatial Correlations of Peak Ground Motions and Response Spectra,” Bulletin of the Seismological Society of America (2008) 98 (1): 354-365.

Gomez, R., and Garcia-Ranz, F. (1988). “The Mexico earthquake of September 19, 1985 -Complementary technical norms for earthquake resistant design, 1987 edition,” *Earthquake Spectra*. 4(3), 441-460.

Instituto de Ingenieria UNAM. (2017). “Reporte preliminar parámetros del movimiento del Suelo sismo de Puebla-Morelos (Mw 7.1) 19 de septiembre de 2017, Ciudad de Mexico.

Rosenblueth, E. (1979). “Seismic Design Requirements in a Mexican 1976 Code,” *Earthquake Engineering and Structural Dynamics*. Vol 7, 49-61.

United States Geological Survey (USGS), 2017. Earthquake Hazards Program, M 7.1 - 1km E of Ayutla, Mexico, available at: https://earthquake.usgs.gov/earthquakes/eventpage/us2000ar20#executive.

The Earthquake Engineering Research Institute (EERI) is a nonprofit corporation. The objective of EERI is to reduce earthquake risk by (1) advancing the science and practice of earthquake engineering, (2) improving understanding of the impact of earthquakes on the physical, social, economic, political, and cultural environment, and (3) advocating comprehensive and realistic measures for reducing the harmful effects of earthquakes.

This publication is available in PDF format from http://www.eeri.org.